JMEPEG (2008) 17:70–79
DOI: 10.1007/s11665-007-9147-7

1059-9495/$19.00

The Impact of Corrosion on the Mechanical Behavior of Welded Splices of Reinforcing Steel S400 and $B500_c$

Ch.Alk. Apostolopoulos, D. Michalopoulos, and L. Dimitrov

(Submitted February 13, 2007; in revised form February 26, 2007)

The reinforcing steel, used in concrete structures, when corroded causes reduction of the strength properties and especially drastic reduction of ductility. Steel corrosion constitutes an important factor of progressive devaluation of its mechanical properties and serious reduction of the integrity of structures. The problem becomes more evident specifically for structures near coastal areas where salt corrosion is predominant. Reinforced concrete columns and beams are quite often extended by welding new steel reinforcement to the already corroded existing steel. In the present article the impact of corrosion on the mechanical properties of welded splices of reinforcing Steel S400 and $B500_c$ is examined. An experimental investigation was conducted and tensile and compressive results are presented for welded precorroded S400 and noncorroded $B500_c$ steel splices. The mechanical behavior of welded splices in tension are different in compression and depend strongly on the level of corrosion of the S400 bars.

Keywords compressive strength, corrosion, elongation to failure, S400 and $B500_c$ steel, tensile strength, welding

1. Introduction

The objective of this article is to investigate the mechanical properties and behavior of the welded splices between new and existing reinforcement of concrete structures during addition of new columns and beams, a practice which is very common during building expansion. In Greece this procedure is performed according to ELOT 971 (Ref 1) standard, using lap-welding joints of the new and existing steel bars in a vertical upward or overhead position. In many instances and in actual practice these specifications are nonapplicable due to space limitations of the required connections. Properly designed and well-executed splices are a key element in the construction industry. The lap splice, when space limitations permit and when it will satisfy all requirements, is generally the most common method for splicing reinforcing bars. When lap splices however, are undesirable or impractical, or when their use is not permitted by the design codes, mechanical or welded connections should be used to splice the reinforcing bars (Ref 2).

S400 known also as BSt420 steel was used extensively in reinforced concrete structures between 1960 and 1992 and later was replaced by S500s. In the last 2 to 3 years the production of an improved steel $B500_c$ was initiated due to the need for higher yield strength steel required in seismogenic regions like Greece, Turkey, and East Bulgarian Coast.

Ch.Alk. Apostolopoulos and **D. Michalopoulos**, Department of Mechanical Engineering and Aeronautics, University of Patras, Patras 26500, Greece; and **L. Dimitrov**, Department of Mechanical Engineering, Technical University of Sofia, Sofia, Bulgaria. Contact e-mail: capostolo@tee.gr.

Figure 1 shows the structure of $B500_c$ steel after treatment in Nital (1.5 to 5 mL concentrated Nitric acid in 100 mL of ethyl alcohol solution) for 5 to 30 s. The hard martensite layer is shown in the outer part, followed by bainite and ferrite-pearlite layers. This type of structure is obtained due to the tempcore method which gives the material additional yield strength caused by the soft central layer and high strength caused by the hard outer layer.

Ribbed reinforcing steel, grade $B500_c$, is produced according to the Greek National Standard ELOT 1421 (Ref 3). The influence of atmospheric corrosion on mechanical properties of reinforcing steels in arid regions has been investigated (Ref 4, 5). The conclusion was that atmospheric corrosion in arid areas does not influence the strength and ductility of reinforcing steels. Further tests specify that the level of reinforcement corrosion does not influence the tensile strength of steel bars, calculated on the actual cross-sectional area. However, when the nominal diameter is utilized in the calculations, the tensile strength is less than the ASTM A 615 requirement (of 600 MPa) when the degree of corrosion was 11 and 24% for 6 and 12 mm diameter steel bars, respectively. Furthermore, reinforcing steel bars with more than 10% corrosion indicate a brittle failure (Ref 5-7).

An analysis was performed on the effect of the type of welding in corrugated bars of two austenitic stainless steels (low-nickel AISI 204Cu and traditional 304 types) and a duplex stainless steel (SAF 2205 type) versus corrosion behavior (Ref 8). Authors pointed out that oxides formed during the welding process reduce the corrosion resistance of steels. The surface of the reinforcements has to be cleaned. The efficiency of the cleaning method depends on the composition of the welded steels and the characteristics of the environment.

Research carried out on corroded reinforced concrete beams showed that the level of corrosion increases both the deflections and the crack widths at service load, and reduces the strength at ultimate load (Ref 9). Besides, corrosion modifies the type of failure in concrete beams with usual ratios of reinforcement. Whereas sound tested beams failed by bending, deteriorated

beams failed by shear. Pitting at links and cracking and spalling of top concrete cover, due to corrosion of reinforcement, have been shown as the most relevant damages in the tested beams.

The transfer of forces through the reinforced concrete steel bars requires relatively long overlap between them, even though in many practical applications, such as older building expansion or beam or column repair, this is not the case and the steel length is rather small. In such instances a rather effective connection method is the lap welding of the existing with the new steel bars thus making the connection suitable for transferring of these forces. The reliable and safe design of these connections is governed by regulatory standards, which require that the weld bead is long enough in order to transfer the forces from one rod to the other. However, the proper welding procedure falls short in many instances due to space limitations or other unpredictable factors (Ref 2, 10). It is questionable therefore if the welded splices can perform as designed and carry safely and reliably the forces for which they were intended.

The welding of reinforcing steel regulations requires that the tensile strength of welded splices should be at least equal to the strength of the steels used, while according to ELOT 971 the tensile strength must be 90% higher than the original strength of the steel used (Ref 1, 11). The main tensile requirement of the existing regulations is related to the tensile strength of the welded joint and no reference is made to the maximum strain or yield strength of the connection (Ref 1, 3, 12-15).

Several experimental investigations of the mechanical properties of S400 steel for different levels of corrosion and also welded splices have been conducted (Ref 10, 16) and the factors influencing their strength behavior are critiqued. An investigation of the effect of carbonation on public buildings located up to 800 m from the seashore has been conducted (Ref 17). The results, based on the analysis of carbonation depth, resistivity, compressive strength, and porosity data suggested that risk of concrete deterioration due to carbonation increases with the distance from the seashore as well as with the elevation. Data from laboratory specimens exposed to the same tropical marine environment for 5 years were used to correlate the findings from public buildings.

The objective of this article is to investigate the mechanical properties, behavior, and merit of the lap-welded splices between new and existing reinforcing bars used in concrete structures during addition of new elements such as columns and beams, a practice which is very common during building expansion. Tensile tests were conducted on noncorroded and also on artificially corroded S400 specimens, prepared and treated for different durations in a specially design salt spray corrosion chamber and on noncorroded $B500_c$ in order to investigate their mechanical properties and tensile behavior. In addition, tensile and compressive tests were also conducted on noncorroded $B500_c$ and on corroded S400 bars, respectively, in order to examine the impact of corrosion on the mechanical behavior of $B500_c$ and S400 welded splices.

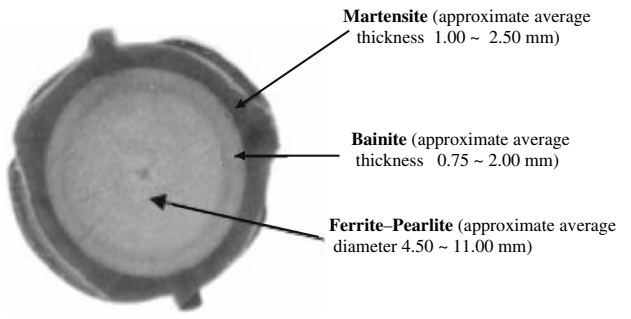

Fig. 1 Internal structure of $B500_c$ steel treated in Nital, for approximately 10 to 20 mm diameter

2. Welding of Reinforcing Steel and Methods

Welding of reinforcing steels strongly depends on their chemical composition. $B500_c$ is a carbon steel with chemical composition shown in Table 1.

S400 is a special type of steel with chemical composition shown in Table 2.

The main parameters that influence welded joints are:

(a) High local temperature, about 1600 °C, with critical values of 900 °C for carbon steel and variation of the steel microstructure and properties in the locality of the weld. At this temperature the ferrite assumes different crystalline shape known as austenite and which is maintained up to 1530 °C which is near the melting point. The presence of hard and brittle constituents that make the steel more fragile depend on the chemical composition and way of production and characterizes its weldability.

(b) Impurities such as sulfur (S), phosphorus (P), sodium (N), hydrogen (H), and oxygen (O) have a negative impact on the weld quality and are responsible for crack development in the steel and welds. Silicon (Si) in quantities of 0.03 to 0.35% improves the weld quality while above 1% it lowers it and manganese (Mn) which is usually below 1% improves it since it traps the sulfur.

The heat-affected zone is of particular importance because of the metallurgical changes that occur in steel during the

Table 1 Chemical percentage composition of $B500_c$ steel, according to ELOT 1421

C	P	S	N	Cu	Carbon equivalent, C_{eq}
0.240	0.055	0.055	0.013	0.800	0.530

Table 2 Chemical percentage composition of S400 steel

C	Mn	S	P	Si	Ni	Cr	Cu	V	Mo	N	C_{eq}
0.350	0.940	0.026	0.013	0.260	0.100	0.160	0.420	0.002	0.023	0.010	0.540

process of welding (heating) and following rapid cooling. A large part of metal within the heating zone has transformed to austenite because of the intensive heat in welding. Upon the subsequent cooling, the properties of the metal within the heat-affected zone are determined by the cooling rates and consequent decomposition of the austenite to ferrite and martensite which looks like small needles as shown in Fig. 2.

Designers should anticipate two main problems in welded joints:

(a) Due to the effect of localized extreme heating and following rapid cooling changes take place in microstructure and mechanical properties of the base metal;
(b) Residual stresses are locked in the weldments as a result of the uneven cooling of the weld deposit.

Weldability of steels vary widely according to their carbon content. Plain low-carbon steels have almost perfect weldability but steels with carbon above 0.3% need special operations such as preheating and postheating. The maximum allowed content of chemical elements in steel for good weldability is shown in Table 3. The effect of these elements in controlling the tendency to form heat-affected zone martensite, and thus cold cracking, is usually expressed as carbon equivalent and is calculated by (Ref 18):

$$C_{eq} = \%C + \frac{\%Mn}{4} + \frac{\%Ni}{20} + \frac{\%Cr}{10} + \frac{\%Cu}{40} - \frac{\%Mo}{50} - \frac{\%V}{10} \quad \text{(Eq 1)}$$

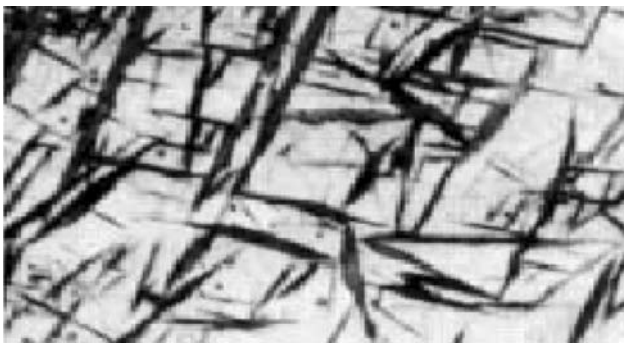

Fig. 2 Martensite particles in a steel. Microscopic inner structure of martensite

where the symbols indicate the % by mass for each element (as determined by means of chemical analysis). For the present case the coefficients for weldability are:

$$\text{S400}: \ C_{eq} = 0.53 \quad \text{(Eq 2)}$$

$$\text{B500}_c: \ C_{eq} = 0.54 \quad \text{(Eq 3)}$$

This is considered as an indication that both steels have good weldability.

The welding methods of structural steel reinforcement and the corresponding types of joints are shown in Table 3. Butt-welded joint is only performed on bars with a diameter ≥20 mm.

In this study, the specimens were welded as shown in Fig. 3 and 4, according to ELOT 971 standard and included corroded S400 steel specimens welded to noncorroded $B500_c$ with two weld beads, on one side only, of 5*d* length and free space of 20 mm in between them. Rutile grade titanium dioxide welding rods, 2.5 mm diameter, were used for the welding process.

3. Experimental Procedure

Tensile tests were conducted on noncorroded and also on artificially corroded S400 specimens, prepared and treated for different durations in a specially design salt spray corrosion chamber and on noncorroded $B500_c$ in order to investigate their mechanical properties and tensile behavior. In addition tensile and compressive tests were also conducted on welded noncorroded $B500_c$ and on corroded S400 bars, respectively, in order to examine the impact of corrosion on the mechanical behavior of $B500_c$ and S400 welded splices.

Table 3 Welding methods

Type of weld joints	Resistance spot welding	Semiautomatic in protective atmosphere CO_2/Ar	Electric arc welding with coated electrodes	Autogenous welding
Cruciform	+	+	+	
Lap		+	+	
Butt		+	+	+

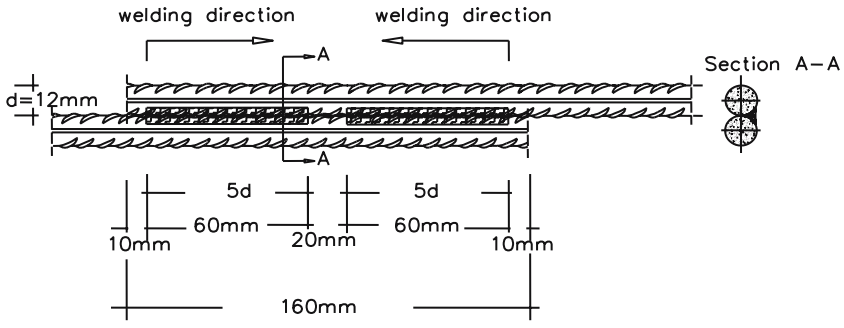

Fig. 3 Schematic of direct lap joint of reinforcing steel specimens

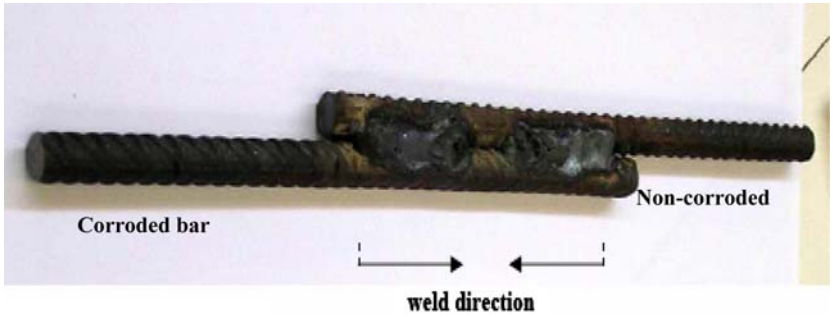

Fig. 4 Welded specimens

Three S400 steel specimens of 12 mm diameter each were artificially corroded in a salt spray chamber for 30, 60, and 90 days duration. Afterwards tensile tests were also conducted on a tensile testing machine by application of force at a rate of 2 mm/min not only on the corroded S400 bars but also on the reference $B500_c$ and S400 specimens, a total of 15 specimens.

Figure 3 shows a schematic of a typical direct lap joint of two parallel reinforcing steel specimens. The welded specimens were subjected to tensile and compressive tests and the corresponding strength and ductility of the connections were examined. A total of 104 specimens were used in this study which were cut with a hard metal disk and prepared to length ≥280 mm and diameter 12 mm. From these 52 specimens were from $B500_c$ steel while the other 52 specimens were from $S400_s$. The noncorroded series of specimens included 12 pieces of S400s steel that were welded with $B500_c$ steel.

A total of 40, S400 12 mm steel specimens, were corroded for 15, 30, 45, and 60 days in a salt spray corrosion chamber. Each corrosion level included five samples, which after corrosion were sanded down with emery cloth to remove the corrosion particles and welded with $B500_c$ and S400 noncorroded steel. In addition noncorroded $B500_c$ were welded with noncorroded S400 bars. The welding procedure was manual using rutile grade titanium dioxide welding rods according to ELOT 971 standard and the welding length was 160 mm. Seven of the noncorroded specimens were tested in tension and five in compression, while each corrosion level included five tension and five compression tests in order to measure their mechanical properties.

Corrosion of the samples was obtained in a salt spray corrosion chamber, according to ASTM B-117-94 standard for the durations shown in Table 4. Table 5 shows the mechanical properties of S400 steel, while Table 6 shows the mechanical properties of $B500_c$.

Table 7 shows the mass loss of the specimens for each corrosion level.

Table 8 shows the welded specimens that were subjected to tensile and compressive tests.

Table 4 S400 corroded steel specimens

Corrosion duration (days)	Number of specimens
15	10
30	10
45	10
60	10

4. Results

Tensile tests were performed in both noncorroded and corroded specimens in order to investigate the impact of corrosion as combined with the welding on the mechanical properties of steel.

Figure 5 shows representative stress-strain diagrams of noncorroded $B500_c$ and S400 and also corroded at various levels S400 steel specimens. It is also shown that even though the noncorroded $B500_c$ surpasses the noncorroded S400 yield point, its maximum strength and strain are lower. A gradual degradation in the strength and ductility properties of the gradually corroded S400 steel are also observed. This type of behavior of the noncorroded S400 and $B500_c$ explains the tensile test result of the welded splice, as it is also explained from the results of Table 10, where while the initial yielding of the S400 is followed by yielding of the $B500_c$ the eventual failure at the $B500_c$ bar is observed. Figure 5 and Table 9 refer to apparent values which means that each of the applied force was divided by the initial nominal cross-sectional area.

Figure 6 illustrates the mode of failure of the welded specimens in tension. Even though the noncorroded $B500_c$ surpasses the noncorroded S400 yield point, its maximum strength and strain are lower. A gradual degradation in the strength and ductility properties of the gradually corroded S400 steel are also observed.

As shown in Fig. 6, a direct correlation appears to exist between material failure and level of ductility. Failures far away and near the welded joint are characterized by high and low ductility level respectively and neck formation of the failed bar.

In the compressive test results, for 60 days corroded S400 and noncorroded $B500_c$ welded splices, was shown that the maximum supported strength and corresponding strain were reduced by 20.50 and 46.50% respectively, Fig. 13, versus the welded joint of the noncorroded bars. The noncorroded S400 and $B500_c$ in the tensile test result of the welded splice is shown in Fig. 7, where the initial yielding of the S400 is followed by yielding and eventual failure of the $B500_c$.

The lap welded splice shown in Fig. 8, besides transferring axial loads $\sigma_x = P_x/A$, causes also two-dimensional bending moments M_y and M_z. Thus the total axial stress is

$$\sigma_x = \frac{P_x}{A} + \frac{M_y}{I_y} \cdot z + \frac{M_z}{I_z} \cdot y \qquad \text{(Eq 4)}$$

In the welded section of the two bars the axial stress σ_x is relatively low since A, I_y, and I_z of the composite section at the

Table 5 Mechanical properties of S400 steel

	Yield strength f_Y, MPa	Fracture strength f_f, MPa	Elongation at tensile strength, %	Elongation to fracture, %	Ratio of fracture to yield stress f_f/f_Y
ELOT 959[a]	≥400	≥500	···	≥14	≥1.05
DIN 488	≥420	≥500	···	10	···

[a]ELOT 959 (Ref 19)

Table 6 Mechanical properties of $B500_c$ steel

	Yield strength f_Y, MPa	Fracture strength f_f, MPa	Elongation at tensile strength, %	Elongation to fracture, %	Ratio of fracture to yield stress f_f/f_Y
ELOT 1421-3	≥500		≥7.5		≥1.15 ≤1.35
EKOS 2000[a]	≥500	≥550	≥7	12	≥1.10 ≤1.30
ELOT 971	≥500	≥550	···	12	≥1.08 1.30
DIN 488 (high ductility)	≥500	≥550	≥5		≥1.05

[a]EKOS 2000 (Ref 20)

Table 7 Mass loss of S400 steel specimens for different corrosion levels

Corrosion duration	Initial mass m_i, kg	Final mass m_f, kg	Mass loss, %
15	274.24	268.77	1.99
30	277.23	265.90	4.09
45	276.31	259.91	5.94
60	272.26	244.92	10.04

Table 8 Welded specimens subjected to tensile and compressive tests

	Welded specimens			
Corrosion duration, days	Tension testing	Compression resting	Corroded specimen	Noncorroded specimen
0	7	7	S400	$B500_c$
15	5	5	S400	$B500_c$
30	5	5	S400	$B500_c$
45	5	5	S400	$B500_c$
60	5	5	S400	$B500_c$

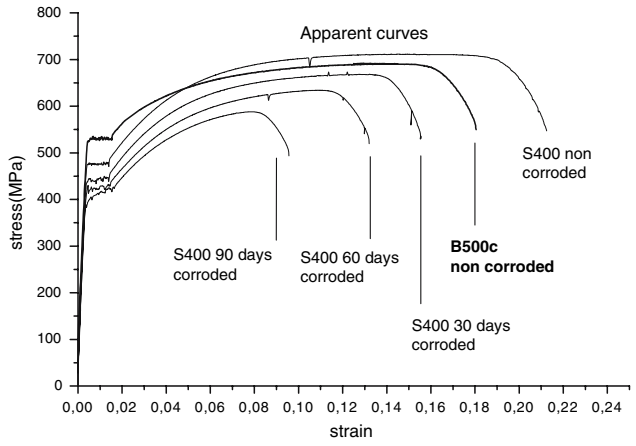

Fig. 5 Representative stress-strain diagrams of noncorroded $B500_c$ and S400 and also corroded at various levels S400 steel specimens

welded portion, including the two bars and the welding bead, are rather high. At points far away from the weld, where the bars stand alone, the corresponding geometry is reduced considerably. In cases of extreme loading followed by failure, considerable contribution of P_x, M_y, and M_z is observed. The usual practice is to approximate $M_y \sim 0.3dP_x$ and $M_z \sim dP_x$, where d is the nominal bar diameter and P_x is the axial force transmitted from one bar to the other (Fig. 9).

Table 10 shows the mechanical tensile and compressive test results of welded splices of noncorroded and corroded S400 and noncorroded $B500_c$ steel specimens, while Table 10 and Fig. 10 show that during tension of the welded joints of noncorroded $B500_c$ and S400, failure will most likely occur on the $B500_c$ bar while the elongation to failure is considerably lower than in the case of failure of the S400 bar.

Figure 10 illustrates tensile tests conducted with noncorroded $B500_c$ steel specimens welded to corroded S400 specimens which were corroded for 0, 15, 30, 45, and 60 days.

Table 9 Mechanical properties of $B500_c$ and S400 steel specimens

Salt spray corrosion	0 days	30 days	60 days	90 days
Material S400				
Apparent YS, MPa	459.08	436.35	413.49	405.01
Apparent UTS, MPa	696.49	669.64	640.41	618.17
Elongation to fracture, %	21.24	15.49	13.15	10.90
Material $B500_c$				
Apparent YS, MPa	540.32			
Apparent UTS, MPa	648.47			
Elongation to fracture, %	18.50			

YS = yield strength, UTS = ultimate tensile strength

Table 10 Tensile and compressive test results of welded splices

	Exposure time, days	Tensile breaking force, kN	Elongation to failure, mm	Failed material	Compressive failure force, kN	Elongation to failure ΔL, mm	Failed material
1	Noncorroded	76.27	27.07	B500c	33.90	5.921	S400
2		76.69	27.97	B500c	34.30	6.811	S400
3		80.40	34.85	S400	32.50	6.043	S400
4		77.95	25.43	B500c	32.95	6.3324	S400
5		77.90	28.37	B500c	33.99	5.53132	S400
	Mean value	$\bar{P} = 77.84$	$\Delta\bar{L} = 28.74$		$\bar{P} = 33.53$	$\Delta\bar{L} = 6.12$	
6	15 days salt spray corrosion on S400	79.12	39.37	S400	30.164	6.36902	S400
7		79.79	36.28	S400	29.095	5.10101	S400
8		78.87	32.51	B500c	26.794	4.89959	S400
9		78.82	36.10	B500c	29.041	5.44281	S400
10		79.91	36.68	S400	29.565	5.3421	S400
	Mean value	$\bar{P} = 79.30$	$\Delta\bar{L} = 36.19$		$\bar{P} = 28.93$	$\Delta\bar{L} = 5.43$	
11	30 days salt spray corrosion on S400	75.88	24.30	B500c	30.258	5.45044	S400
12		76.81	30.77	S400	30.371	4.70276	S400
13		76.79	29.63	B500c	28.61	4.75769	S400
14		77.35	31.75	S400	29.791	4.03595	S400
15		77.27	31.73	S400	31.784	4.99572	S400
	Mean value	$\bar{P} = 76.82$	$\Delta\bar{L} = 29.63$		$\bar{P} = 30.16$	$\Delta\bar{L} = 4.78$	
16	45 days salt spray corrosion on S400	73.43	22.74	B500c	33.04	5.18951	S400
17		74.31	22.21	S400	30.029	3.92456	S400
18		74.19	22.20	S400	27.191	3.6499	S400
19		74.83	30.34	S400	30.41	5.55572	S400
20		74.51	22.45	S400	29.376	4.10461	S400
	Mean value	$\bar{P} = 74.25$	$\Delta\bar{L} = 23.98$		$\bar{P} = 30.0$	$\Delta\bar{L} = 4.48$	
21	60 days salt spray corrosion on S400	71.59	14.81	S400	28.113	3.21287	S400
22		70.77	16.69	S400	29.371	4.5573	S400
23		70.96	15.74	S400	26.511	2.41999	S400
24		69.84	11.70	S400	24.925	2.60959	S400
25		68.64	15.78	S400	24.098	3.57138	S400
	Mean value	$\bar{P} = 70.36$	$\Delta\bar{L} = 14.94$		$\bar{P} = 26.6$	$\Delta\bar{L} = 3.27$	

Fig. 6 Illustration of the tensile mode of failure of welded specimens

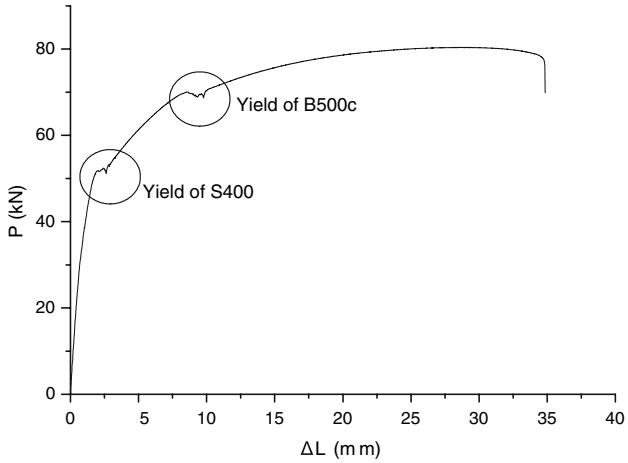

Fig. 7 Tensile test of welded splice S400 and $B500_c$ of noncorroded steel specimens versus strain behavior

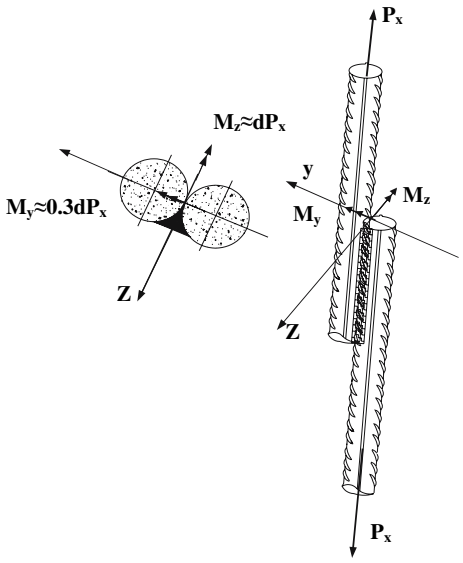

Fig. 8 Welded splice of steel bars

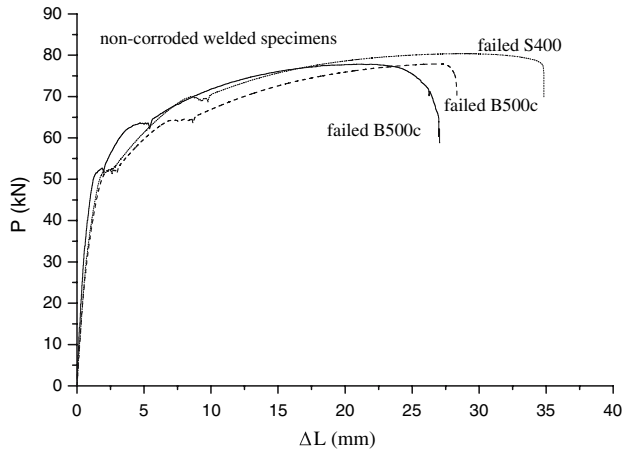

Fig. 9 Tensile tests for welded splices of noncorroded specimens ($B500_c$ steel welded with S400)

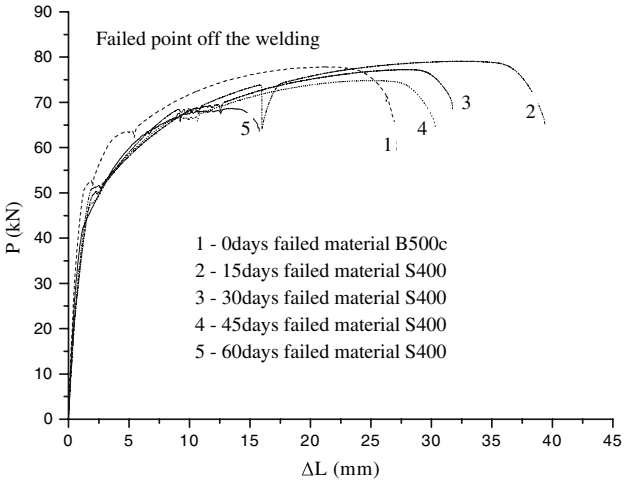

Fig. 10 Tensile tests for noncorroded $B500_c$ steel specimens welded to corroded S400 steel specimens which have been corroded for 0, 15, 30, 45, and 60 days

It can be observed that as the corrosion level increases the failure level and the elongation of the welded connections decrease.

Figure 11 illustrates the compressive mode of failure of the welded splice caused by bending of the bar with the lower yield point which in this case is the S400.

Figure 12 shows a typical compressive force versus strain behavior diagram for $B500_c$ and S400 steel welded joint.

Figure 13 shows the compressive force versus strain of S400 steel bars corroded for 15, 30, 45, and 60 days and welded to noncorroded $B500_c$ bars. It is indicated that the higher the corrosion level the lower the strength and ductility of the connection. Tests indicated that the corrosion duration is related to the reduction in strength of the welded joint. The failed material was the corroded S400 steel bar.

Figures 14 and 15 show the tensile and compressive force behavior of the lap welded joints indicating the variation of the maximum force and elongation to failure for different corrosion levels, and which were fitted by the following regression polynomial:

$$y = A + B_1x + B_2x^2 + B_3x^3 \quad \text{(Eq 5)}$$

In Fig. 14 the tensile constants are:

$$A = -77.91257,\ B_1 = 0.19730,\ B_2 = -0.00925 \text{ and } B_3 = 6.46914\text{E} - 5$$

And the compressive constants are:

$$A = -33.42429,\ B_1 = 0.53557,\ B_2 = -0.02043,\ B_3 = 2.23704\text{E} - 4.$$

While in Fig. 15 the tensile constants are:

$$A = -29.01457,\ B_1 = 0.85286,\ B_2 = -0.03378,\ B_3 = 2.62222\text{E} - 4$$

Fig. 11 Compressive failure of welded of S400 corroded specimens welded to $B500_c$ noncorroded bars

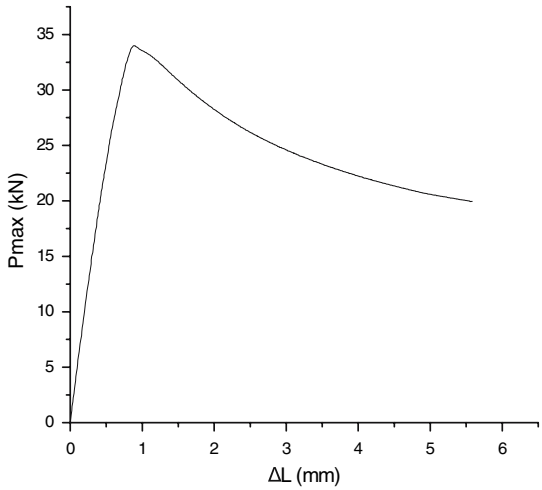

Fig. 12 Compressive force versus strain behavior for $B500_c$ steel welded with S400

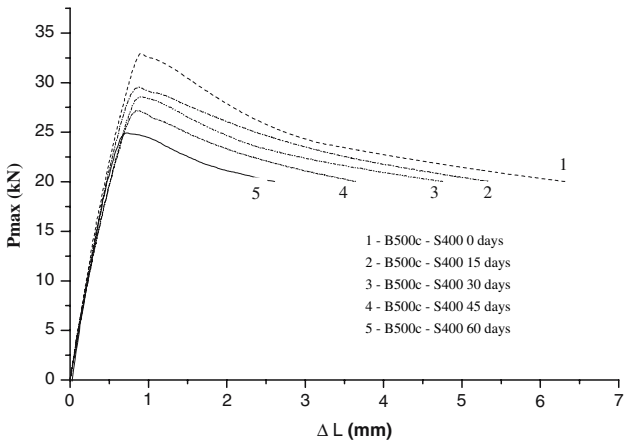

Fig. 13 Compressive force versus strain of $B500_c$ noncorroded steel welded with S400 specimens corroded for 0, 15, 30, 45, and 60 days

And the compressive constants are:

$$A = -6.14243,\ B_1 = 0.07658,\ B_2 = -0.00189,$$
$$B_3 = 2.34568\text{E} - 5.$$

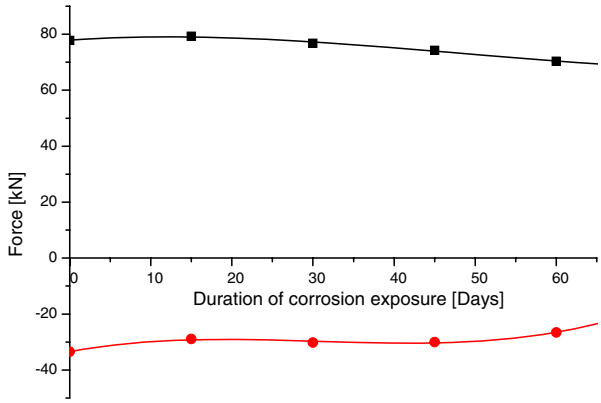

Fig. 14 Tensile and compressive maximum force behavior of lap welded joints

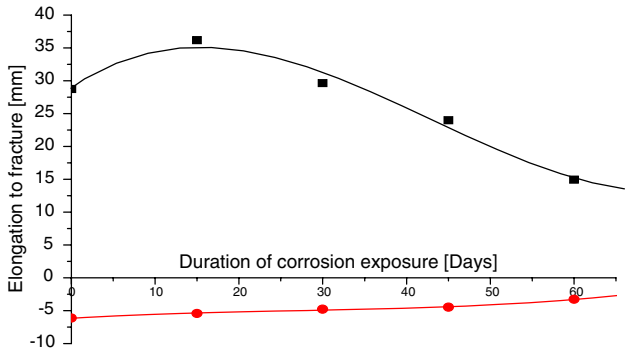

Fig. 15 Tensile and compressive elongation to failure behavior of lap welded joints

Figure 10 illustrates tensile tests conducted with noncorroded $B500_c$ steel specimens welded to S400 bars which were corroded for 0, 15, 30, 45, and 60 days. It is observed that as the corrosion duration increases the failure was due to the inability of the corroded S400 to carry higher loads than the noncorroded $B500_c$.

From the five tensile tests on the welded splices between S400 and $B500_c$ specimens:

(a) For the noncorroded specimens failure occurred once in the S400 and four times in the $B500_c$ bars,

(b) For the 15 and 30 days salt spray corroded S400 specimens, with corresponding mass loss of 1.99 and 4.09%, respectively, failure occurred twice in the $B500_c$ and three times the S400 bars,
(c) For the 45 days salt spray corroded S400 specimens, with corresponding mass loss of 5.94%, failure occurred once in the $B500_c$ bar and four times in the S400 bars, and
(d) For the 60 days salt spray corroded S400 specimens, with corresponding mass loss of 10.00%, all five failures occurred in the S400 bars, with considerable corresponding reduction of the elongation to fracture.

Figures 9, 10 and Table 10 even though they show randomized experimental results, it is clear that in the case that the failure is due to $B500_c$ specimen, the elongation to failure of the welded splice is reduced since this material has lower strain capacity than the S400, which is also shown also in Fig. 5. The reduction in elongation to failure is even greater when failure occurs very close to the weld.

From the tensile tests shown in Table 10 it is concluded that even though the average strength of the welded splice is reduced by 4.60% for 45 days salt spray corrosion of the S400 steel and by 9.60% at 60, the corresponding elongation to failure is reduced by 16.50 and 48.00%, respectively. On the contrary for 15 days corrosion of the S400 steel the tensile strength increases by 1.90% and the elongation to failure increases by 26% since the failed material is closer to S400 which in order to fail absorbs the total uniform strain of both S400 and $B500_c$ steel specimens since the tensile strength of both materials is almost the same, since the 1.90% can be considered as statistical error.

Even though failure of specific material and actual failure location during tensile testing are unpredictable and uncertain, since it depends on the corrosion level of the S400, during compression testing failure occurs always in the S400 specimen due to lower yield point. During tensile testing the failure location is almost unaffected by the maximum fracture force but it is of particular importance for the maximum elongation to failure.

Corrosion duration and mass loss were found to be very important for the integrity of steel and pitting became evident after a few days of salt spray and became progressively more severe as the corrosion level increased. As the steel surface became rougher cavities and notches were formed which made the steel surface locally of smaller diameter than the average value and thus developed stress concentration points which are highly localized at imperfections and especially in the pits and notches of the rib bases of the corroded steel.

A careful examination of Table 10 shows that the approximate maximum applied force and elongation level do not follow a repeatable pattern. This implies that in actual practice careful use of stirrups is necessary, in order to reduce the free bending length during compression, and which could possibly correct the problem. In any case the maximum tensile and compressive loads and the corresponding maximum elongations differ considerably to such a degree that could possibly lead reinforced concrete elements, loaded under intense bending, to unpredictable behavior.

The complex tensile or compressive behavior of welded splices must be given special attention during design of reinforced concrete structures with different types of reinforcing steel in addition to reevaluation of present design practices. Existing design codes treating complex tensile or compressive behavior of welded splices must be reevaluated and engineers involved in the design of reinforced concrete structures with different types of reinforcing steel, must be informed of the importance of such connections, especially in earthquake prone areas.

5. Conclusions

The effect of corrosion and the lap-welded splicing on the mechanical characteristics of maximum sustained load and elongation at maximum force between new and existing reinforcement of concrete structures during addition of new columns and beams, has shown that:

1. Lap-welded joints of noncorroded S400 and $B500_c$ steel bars in tension will most likely fail on the $B500_c$ specimen. However, an increase in corrosion level of S400 will transfer the failure on the corroded bar. In addition and even though the maximum sustained force presents a small reduction the elongation at maximum force is reduced considerably.
2. Lap-welded joints of corroded and noncorroded S400 with noncorroded $B500_c$ steel bars in compression, will always fail on the S400 specimen.
3. Great discrepancy in the behavior of the lap-welded splices was observed between maximum sustained load and maximum elongation to failure.
4. Corrosion and lap welding of reinforcing steel are the main reasons for the degradation of the mechanical characteristics, the behavior of which varies according to the material, the location of failure and the maximum elongation.
5. A reevaluation of the existing design codes, treating complex tensile or compressive behavior of welded splices, is appropriate.

Further investigation is required on the welding methods in order to promote and secure the safety of reinforced concrete structures and especially during expansion and addition of new elements.

References

1. "Weldable Steels for the Reinforcement of Concrete," *ELOT 971*, *Hellenic standard*, Athens, 1994
2. C.A. Issa, An Experimental Study of Welded Splices of Reinforcing Bars, *Building and Environment*, 2006, **41**(10), p 1394–1405
3. "Steel for the Reinforcing of Concrete—Weldable Reinforcing Steel—Part 3," *ELOT 1421-3*, *Hellenic standard*, Technical class $B500_c$, Athens, 2005
4. A.M. Ibrahim, Maslehuddin, H. Saricimen, and A.I. Al-Mana, Influence of Atmospheric Corrosion on the Mechanical Properties of Reinforcing Steel, *Construction and Building Materials*, 1994, **8**(1), p 35–41
5. A.A. Almusallam, Effect of Degree of Corrosion on the Properties of Reinforcing Steel Bars, *Construction and Building Materials*, 2001, **15**(8), p 361–368
6. Ch. Alk. Apostolopoulos, Mechanical Behavior of Corroded Reinforcing Steel Bars $S500_s$ Tempcore Under Low Cycle Fatigue, *Construction and Building Materials*, 2007, **21**, p 1447–1456

7. Ch. Alk. Apostolopoulos, M.P. Papadopoulos, and Sp.G. Pantelakis, Tensile Behavior of Corroded Reinforcing Steel Bars BSt 500s, *Construction and Building Materials*, 2006, **20**(9), p 782–789
8. A. Bautista, G. Blanco, F. Velasco, and M.A. Martinez, Corrosion Performance of Welded Stainless Steels Reinforcements in Simulated Pore Solutions, *Construction and Building Materials*, 2007, in press
9. J. Rodriguez, L.M. Ortega, and J. Casal, Load Carrying Capacity of Concrete Structures with Corroded Reinforcement, *Construction and Building Materials*, 1997, **11**(4), p 239–248
10. S. Dritsos and K. Pilakoutas, Strengthening Existing RC Structures by Additional Reinforcement, *Proc. of International Conference on Rehabilitation, Renovation and Repairs of Structures*, Visakhapatnam, India, 1994, p 112–119
11. "Welding of Reinforcing Steel," *pvEN ISO 17660*, 2002
12. "Reinforcing Steel Grades, Properties Marking," *DIN 488*, 1984
13. "Metal Arc Welding of Steel for Concrete Reinforcement," *CEN 247/BS 7123*, 1989
14. "Structural Welding Code, Reinforcing Steel," *ANSI/AWS D1*, 4, 1992
15. "Welding of Reinforcing Bars in Reinforced Concrete Structures," *W186-M 1990*, 1998
16. C. Apostolopoulos and M. Papadopoulos, Tensile and Low Cycle Fatigue Behavior of Corroded Reinforcing Steel Bars S400, *Construction and Building Materials*, 2005, **21**(4), p 855–864
17. P. Castro, E.I. Moreno, and J. Genescá, Influence of Marine Micro-Climates on Carbonation of Reinforced Concrete Buildings, *Cement and Concrete Research*, 2000, **30**(10), p 1565–1571
18. B. Niebel, A. Draper, and R. Wysk, Modern Manufacturing Process Engineering, McGraw-Hill, 1989, p 639
19. "Steels for the Reinforcement of Concrete," *ELOT 959*, *Hellenic Standard*, Athens, 1994
20. "Hellenic Standard for Reinforced Concrete," *EKOS 2000*, Athens, 2000